Süleyman Demirel Üniversitesi
Fen Bilimleri Enstitüsü Dergisi
Cilt 28, Sayı 2, 197-206, 2024

Süleyman Demirel University
Journal of Natural and Applied Sciences
Volume 28, Issue 2, 197-206, 2024

DOI: 10.19113/sdufenbed.1496941

Non-Isolated Bidirectional DC-DC Converter Design and Low Power Application for EV Charging Station

Furkan Üstünsoy*[1], H. Hüseyin Sayan[2], Sadık Yıldız[3]

[1,3] Gazi University, Institute of Natural and Applied Sciences, 06560, Ankara, Turkey
[2] Gazi University, Faculty of Technology, Electrical-Electronic Engineering, 06560, Ankara, Turkey

(Alınış / Received: 06.06.2024, Kabul / Accepted: 10.07.2024, Online Yayınlanma / Published Online: 23.08.2024)

Keywords
EVs charging,
DC/DC converter,
V2V,
V2G

Abstract: Today, the negative impact of charging on the grid is becoming a major concern as the number of electric vehicles increases. The charging topologies such as V2G, V2H and V2V are being studied to solve this problem. The most critical issue in this context is the design and use of appropriate infrastructure and equipment. In this study, firstly a low-cost and high-efficiency non-isolated bidirectional 120W DC-DC converter suitable for DC charging stations is designed. The designed converter was analysed both by analytical methods and by operating at low powers. Secondly, a real-world implementation of V2V and V2H topologies has been performed using these designed converters. In the application study, a DC charging station model was created by using 4 of these converters as charging units. The 90-minute operation of the designed charging station was realised according to a rule-based algorithm. Accordingly, it has been shown that the efficiency of the non-isolated bidirectional DC-DC converter designed is 95%. It is also proved that 54.16% of the EVs load can be shifted to off-peak time period using V2V topology in real world application. According to the results, it is understood that the isolated and high-power version of the designed converter is suitable for charging stations.

EA Şarj İstasyonu için İzolesiz Çift Yönlü DA-DA Dönüştürücü Tasarımı ve Düşük Güçlü Uygulaması

Anahtar Kelimeler
EA' ların şarjı,
DA/DA dönüştürücü,
V2V,
V2G

Özet: Günümüzde elektrikli araçların sayısı arttıkça şarjın şebeke üzerindeki olumsuz etkisi büyük bir endişe kaynağı haline geliyor. Bu sorunu çözmek için V2G, V2H ve V2V gibi şarj topolojileri üzerinde çalışılmaktadır. Bu bağlamda en kritik konu uygun altyapı ve ekipmanların tasarlanması ve kullanılmasıdır. Bu çalışmada öncelikle DA şarj istasyonlarına uygun, düşük maliyetli ve yüksek verimli, izolasyonsuz çift yönlü 120 W DA-DA dönüştürücü tasarlanmıştır. Tasarlanan dönüştürücü hem analitik yöntemlerle hem de düşük güçlerde çalıştırılarak analiz edilmiştir. İkinci olarak, tasarlanan bu dönüştürücüler kullanılarak V2V ve V2H topolojilerinin gerçek dünyada uygulanması gerçekleştirildi. Uygulama çalışmasında bu dönüştürücülerden 4 tanesi şarj ünitesi olarak kullanılarak DA şarj istasyonu modeli oluşturulmuştur. Tasarlanan şarj istasyonunun 90 dakikalık çalışması kural tabanlı bir algoritmaya göre gerçekleştirilmiştir. Buna göre tasarlanan izolasyonsuz çift yönlü DA-DA dönüştürücünün veriminin %95 olduğu gösterilmiştir. Ayrıca, gerçek dünya uygulamasında V2V topolojisi kullanılarak EV yükünün %54.16'sının yoğun olmayan zaman dilimine kaydırılabileceği kanıtlanmıştır. Sonuçlara göre tasarlanan dönüştürücünün izoleli ve yüksek güçlü versiyonunun şarj istasyonları için uygun olduğu anlaşılmıştır.

1. Introduction

The use of electric vehicles (EVs) in transportation is growing rapidly worldwide due to environmental factors and concerns about the depletion of fossil fuels. The rapid spread of EVs raises different concerns. The

* Corresponding author: ustunsoy.furkan@gmail.com

biggest threat to the expansion of EVs is the creation of power quality problems for the grid. Harmonics, reactive power, voltage drops and fluctuations, grid frequency instabilities, unbalanced loads, etc. could be given as examples of power quality problems caused by the charging process. Most of these problems can be largely solved within the charging station by simple hardware precautions in the design of the charging block. However, the voltage and frequency instability of the main grid is a very complex and difficult problem to solve. The main reason for this problem is the disruption of the balance between energy supply and demand. In this case, unlimited expansion of the production-transmission-distribution infrastructure is not a wise solution. For this reason, researchers have conducted numerous studies in recent years on intelligent charging strategies using charging topologies such as V2G (vehicle-to-grid), V2H (vehicle-to-home), or V2V (vehicle-to-vehicle) [1,2]. The applicability of these proposed strategies in the real world is another area of research for researchers. Today's chargers use unidirectional energy flow for both fast and slow charging. However, in the future, when the number of EVs reaches the current number of conventional vehicles, the use of these proposed strategies will be inevitable. For this reason, especially slow charging blocks should be designed for bidirectional energy flow. In this study, a high efficiency non-isolated bidirectional DC-DC converter for bidirectional energy flow is designed. Both simulation and implementation of the designed bidirectional DC-DC converter have been implemented.

There are many studies in the literature on the design of non-isolated bidirectional DC-DC converters. For example, in [3], the characteristics of current and future trends of non-isolated converters including buck-boost, single-ended primary inductor, Cuk, z-source, zeta and hybrid DC-DC converters are highlighted based on performance parameters. In [4], the design and control of a multiphase gap bidirectional DC-DC converter was carried out. In [5], a bidirectional DC-DC converter (BDC) is proposed for the EV application. In [6], a bidirectional, non-isolated, hybrid modular DC-DC converter for high voltage (HV) applications is investigated. Another study presents a bidirectional DC-DC converter with dual input ports for Hybrid Energy Storage System (HESS) [7]. The study [8] focuses on the modified structure of power electronic interfaces with four non-isolated ports (two input and two output ports) that can be used in electric vehicle (EV) applications. Another study provides a comprehensive review of non-isolated bidirectional DC-DC converter topologies [9]. In [10], a simpler, non-isolated, bidirectional DC-DC converter based on logic control circuits is proposed for both battery and supercapacitor topologies. Another study proposes an improved non-isolated single inductor multiple input buck DC-DC converter with reduced component count [11]. In [12], a new bidirectional multi-port DC-DC converter that can be operated in both step-up and step-down modes is introduced, which is recommended for EV applications. In another study, an advanced controller for multi-input bidirectional DC-DC power converter for hybrid energy storage system (HESS) is presented [13]. In [14], a new non-isolated bidirectional DC-DC converter with free ripple input current and zero voltage switching (ZVS) capability is proposed. In another paper, a new integrated cascade bidirectional DC-DC converter is presented to optimize a central charge balancing system [15]. In [16], the performance analysis and comparison of two types of bidirectional DC-DC converters, a step-down-booster capacitor in the middle and a step-down-step-up inductor in the middle, for use in EVs are presented. Another study discussed a possible EV configuration based on supercapacitors and batteries using a bidirectional DC-DC converter to provide reliable and fast energy transfer [17]. In [18], a new topology for high stage multiport DC-DC converters is proposed. In [19], soft-switching topologies for non-isolated DC-DC converters are introduced and the classification and characteristics of all types of soft-switching technologies are presented. In another study, a bridgeless Cuk-derived DC-DC converter for V2V charge transfer as an on-board charger was designed and analyzed [20]. In [21], a high-gain non-isolated DC-DC partial power converter for automotive applications was presented.

Valuable work on non-isolated bidirectional/unidirectional DC-DC converters and the operation of topologies such as V2V, V2G, V2H has been presented above. In this paper, the following contributions to the literature are presented.

- A low cost and high efficiency non-isolated bidirectional DC-DC converter is designed and experimental results are presented.
- A low power real charging station architecture for V2V topology is designed for the first time.
- For the first time, it is proved that energy flow between vehicles can be provided in a stable manner using V2V topology.
- For the first time, the real-world applicability of these topologies has been demonstrated.

This paper is organised in five sections. Section 2 presents the designed DC-DC converter circuit topology and simulation results, Section 3 presents the converter board design and efficiency calculation, Section 4 presents the operation of the V2V topology and Section 5 presents the conclusions.

2. Non-Isolated Bidirectional DC-DC Converter Circuit Topology and Simulation Results

Bidirectional DC-DC converters are also referred to in the literature as half-bridge synchronous DC-DC converters. There are two modes for this converter topology. The first is Buck mode, where energy flows from input to output. The second is Boost mode, where energy is transferred from the output to the input. Figure 1 shows the topology of a bidirectional DC-DC converter.

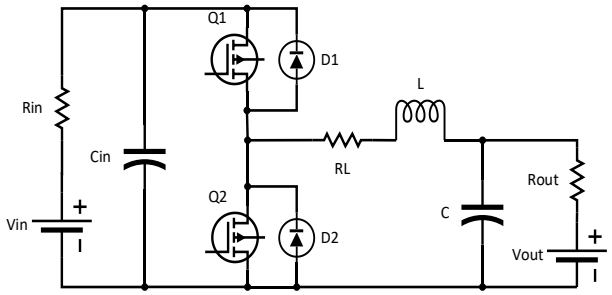

Figure 1. Non-isolated half-bridge bidirectional DC-DC converter

In the topology in Figure-1, MOSFET Q1 and diode D2 are open, MOSFET Q2 and diode D1 are closed for Buck mode. In boost mode, Q2 MOSFET and D1 diode are open, Q1 MOSFET and D2 diode are closed.

The main purpose of DC to DC power conversion is to provide bidirectional energy flow between two different voltage levels under normal and abnormal conditions [22]. In the topology shown in Figure 1, the half-bridge DC-DC power converter operates bidirectionally in step-down and step-up modes. This means that the energy transfer is controlled from low voltage to high voltage and vice versa. Therefore, the performance of the bidirectional DC-DC converter should be analyzed in 2 different modes (Buck-Boost).

2.1 Buck mode

In a bidirectional DC-DC converter topology, Vin is always greater than Vout. Therefore, Buck mode is active for the energy flow from input to output. The relations between input and output for buck mode are given in Equation-1, Equation-2, and Equation-3.

$$\frac{Vout}{Vin} = \frac{Iin}{Iout} = D \tag{1}$$

$$\Delta Iout = \frac{(1-D).Ts.Vout}{L}, \quad L = \frac{(1-D).R_{out}}{2f} \ \ (for\ \Delta Iout = 2I_L) \tag{2}$$

$$\Delta Vout = \frac{Vout(1-D).Ts^2}{8LC}, \quad C = \frac{(1-D).Ts^2}{16L} \ (for\ \Delta Vout = 2Vout) \tag{3}$$

- V_{in} = Input voltage.
- V_{out} = Output voltage.
- I_{in} = Input current.
- I_{out} = Output current.
- D = Transmission Rate.
- ΔI_{out} = Output current ripple.
- ΔV_{out} = Output voltage ripple.
- T_s = Switching period.

In buck mode, MOSFET Q1 and diode D2 are on, MOSFET Q2 and diode D1 are off. When Q1 is in conduction, the inductor (L) and capacitor (C) are charged, and when Q1 is in cut-off state, the charged L and C complete their energy through the D2 diode. In this way, energy flows from the high voltage side to the low voltage side.

2.2 Boost mode

Boost mode is active when power is flowing from the output source to the input. The input-output relationships for boost mode are shown in Equation-4, Equation-5, and Equation-6.

$$\frac{Vout}{Vin} = \frac{Iin}{Iout} = \frac{1}{1-D} \tag{4}$$

$$\Delta Iout = \frac{(1-D).D.Vout}{L.f}, \quad L = \frac{D(1-D)^2.R}{2f} \ (for\ \Delta Iout = 2I_L) \tag{5}$$

$$\Delta Vout = \frac{Iout.D}{C.f}, \quad C = \frac{D}{2fR_{out}} \ (for\ \Delta Vout = 2Vout) \tag{6}$$

- I_L = Inductor current.
- f = Switching frequency.

In boost mode, Q2 MOSFET and D1 diode are on, Q1 MOSFET and D2 diode are off. When Q2 is conducting, L is charging, and when Q2 is disconnected, the voltage on L is reversed because the polarity of IL cannot change immediately. This results in a higher voltage at the junction of mosfets Q1 and Q2 than at the input voltage. In this case, diode D1 is conducting. In this way, energy flows from the low-voltage side to the high-voltage side. The switching and current graphs for buck mode, boost mode, and the transition from buck to boost mode are shown in Figure 2.

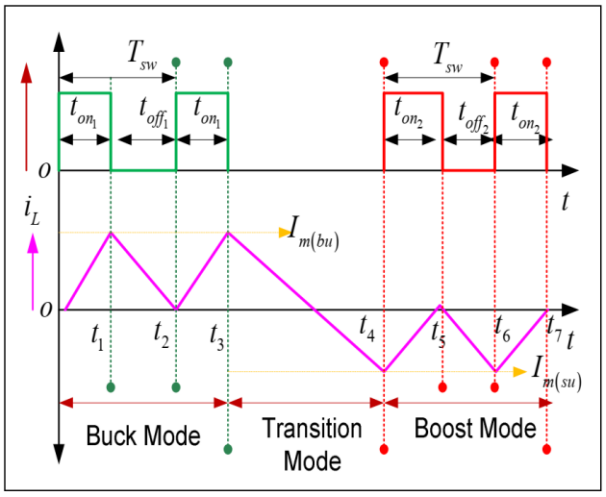

Figure 2. Switching and current graph for transition from buck mode to boost mode [23]

2.3 Non-Isolated bidirectional DC-DC converter simulink model

The Simulink model of a non-isolated bidirectional DC-DC converter was created to analyze the behavior of the designed circuit model.

The circuit model was tested in two different modes and the results were analyzed. Lithium-ion batteries of 12 V-5Ah and 6 V-5ah were used in the model.

The energy flow between these two batteries is controlled by using a PID controller with a constant current reference value (I_{ref}). The Simulink model of the designed circuit is shown in Figure 3. I_{ref}=1.2 A, V_{in}=12 V, V_{out}=6 V and f=15 kHz are set for buck mode. I_{ref}=-1.2A, V_{in}=12V, V_{out}=6V and f=15 kHz are set for boost mode.

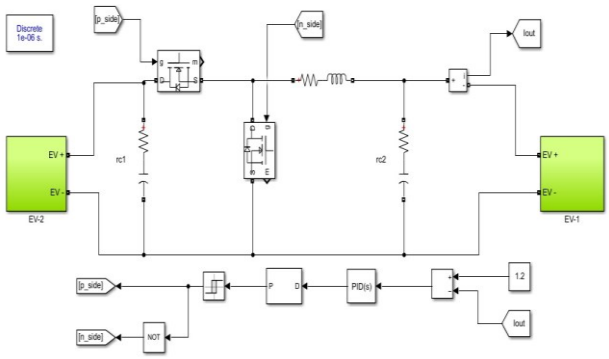

Figure 3. Non-isolated half-bridge bidirectional DC-DC converter simulink model

In the designed Simulink model, the MOSFET values are determined according to the IRFZ 44N MOSFET data. Inductance and capacitor values are also adjusted by considering the values of the elements used in the application circuit.

According to the simulation results for buck mode, the changes of current, voltage and SOC values on the low voltage side are shown in Figure 4 (a). For boost mode, the changes in current, voltage and SOC values on the low voltage side are shown in Figure 4 (b).

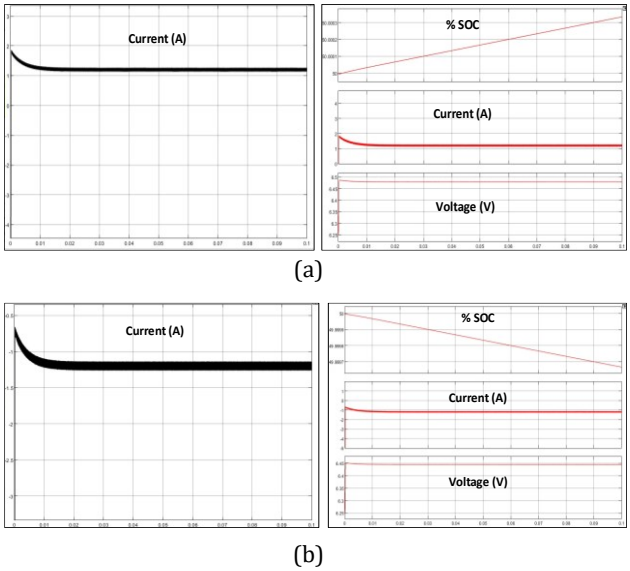

Figure 4. (a) Simulation results for buck mode (b) Simulation results for boost mode

When Figure 4 are analyzed, it is clear that the current ripple ratio is higher in boost mode operation. However, considering the average current value, it is understood that the reference current value is reached in a very short time without error in both buck and boost mode operation. However, due to the internal resistance of the battery, it was observed that the voltage at the battery terminals increased slightly in buck mode and decreased slightly in boost mode during charging. However, it is seen that this voltage value remains stable during charging.

3. Non-Isolated bidirectional DC-DC converter design

In the design, the optimum values of the coil and capacitor for D=0.33 (V_{out}=4 V, V_{in}=12V), f=15 kHz, R_{out}=1.0 Ohm fixed load and I_L=4 A were calculated as L>23.33 µH and C>7.97µF. These values were calculated for ideal conditions. In other words, considering many values such as source resistance, all cable resistances, Vds voltages of power MOSFETs, inductor internal resistance, capacitor resistance, the selected power coil and capacitor values are much higher. The selected power coil and capacitor values are L=100 µH and C=1000 µF. The input voltage and current of the circuit are maximum 48V and 2.5A. Therefore, the power of the bidirectional converter presented is 120 Watt.

The board was designed using IRFZ 44N power MOSFETs, IR 2110 driver, 10 amp 0.1 mH power coil, 7812 and 7805 for driver and optocoupler supply. The schematic circuit model of the designed power card is shown in Figure 5, and the PCB layout is shown in Figure 6.

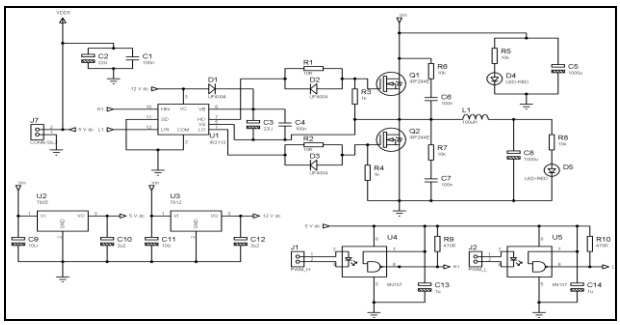

Figure 5. Non-isolated half bridge synchronous DC-DC converter schematic circuit model

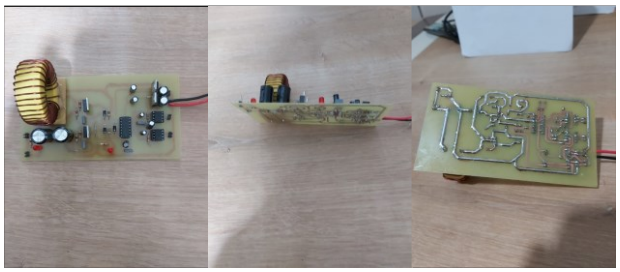

Figure 6. DC-DC converter power card

3.1 Calculation of the efficiency

The designed circuit was operated at D=0.5 and f=15000 Hz for R_{out}=1.0 Ω load. According to this; Output data: V_{out}=4.55V, I_{out}=4.08A, input data: V_{in}=12.51V, I_{in}=1.53A were measured with a multimeter. Since the ammeter is connected in series with the circuit and the load resistance is very low, the internal resistance of the ammeter has little effect on the circuit characteristics. The efficiency calculation is based on actual values. Efficiency is expressed as the ratio of output power to input power as a percentage in Equation 7.

$$\%\eta = \frac{V_{out} \times I_{out}}{V_{in} \times I_{in}} \times 100 = \frac{P_{out}}{P_{in}} \times 100 \qquad (7)$$

- %η = Efficiency in percent.
- P_{out} = Output Power.
- P_{in} = Input Power.

The efficiency of the designed circuit is calculated to be approximately 95%. Oscilloscope outputs for the designed inverter at R_{out}=1.0 kΩ, D=0.4, and f=15000 Hz frequency are shown in Figure 7. Oscilloscope measurements were taken over the resistance on the load.

The STM32F407 microcontroller board is used for closed loop operation of the designed non-isolated half-bridge synchronous DC-DC converter. High-level coding was done using the CubeMX program and TrueStudio program with microcontroller. The control of the designed converter is realized with PWM signals according to the values measured by the Ina219 current-voltage sensor. The test of the designed closed-loop software was performed according to the reference voltage values. The results were monitored in the StmStudio program, which can be recorded and displayed in real time. The output voltage changes of the circuit board according to the references are shown in Figure 8. The output current control of the power board was implemented using the same control architecture. Since batteries are used on both the high and low voltage side, the voltage remains constant. Therefore, current control is sufficient for power flow.

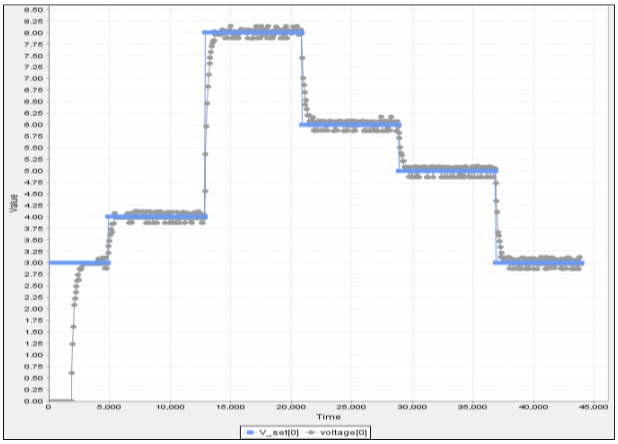

Figure 8. Converter output voltage change measured with the StmStudio program

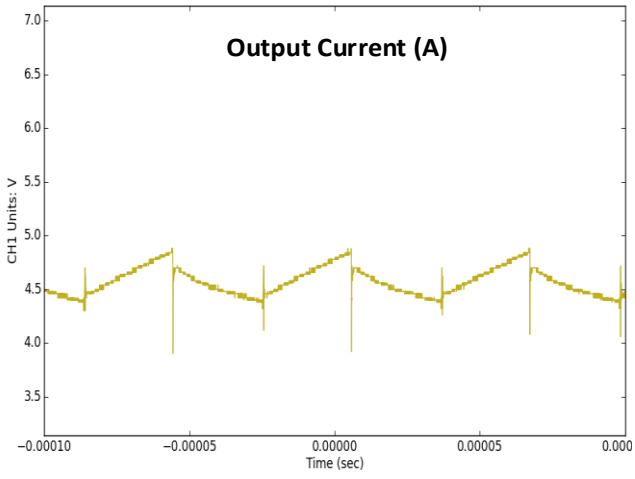

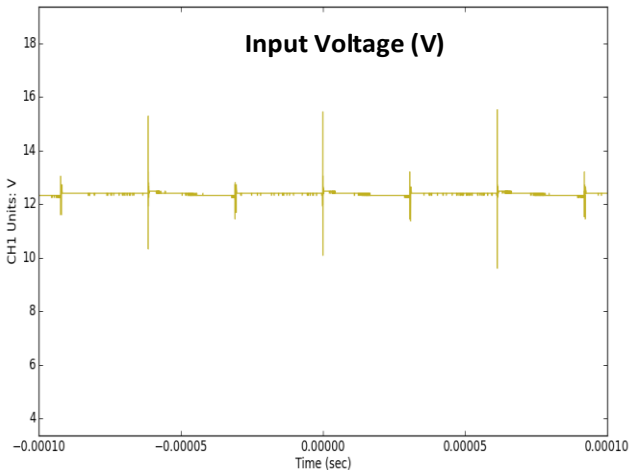

4. Charging Station Design and Low Power Application for V2V Topology

When the studies in the literature are examined, the applicability of V2V topology for DC charging station architecture has not been tested. For this reason, a low power model with 4 charging modules was designed in the laboratory environment to demonstrate the behaviour of the real DC charging station architecture when the V2V topology is operated. The station is controlled according to the charging coordination equations in Reference [1]. Accordingly, Equation 8 refers to the instantaneous power control of vehicles labelled as consumers and Equation 9 refers to the instantaneous power control of vehicles labelled as prosumers.

$$P_{EVJ} = \frac{EPA_j/f_k}{T_s}, P_{EVJ} = I.V_{EVJ}, Iref_{EVJ} = \frac{P_{EVJ}}{V_{EVJ}} \quad (8)$$

$$P_{EVJ} = \frac{(-ECA).f_k}{T_s}, P_{EVJ} = I.V_{EVJ}, Iref_{EVJ} = \frac{P_{EVJ}}{V_{EVJ}} \quad (9)$$

Where EPA (Equation 10) is the total instantaneous energy produced and ECA (Equation 11) is the total instantaneous energy consumed. T_s is the balancing time of the charging levels of all vehicles and is given in Equation 12.

$$EPA_J = [SOC_{EVJ}(t) - SOC_B].C_{Pj} \quad (10)$$

$$ECA_J = [SOC_B - SOC_{EVJ}(t)].C_{Pj} \quad (11)$$

Here, C_{Pj} is the battery capacity of the vehicles and SOC_B is the balance value determined for the charge level. In this study, SOC_B was set to 0.8.

$$T_s = \left| \frac{\sum_{j=1}^{np} EPA_j/f_k - \sum_{j=1}^{nc} ECA_J.f_k}{P_T} \right| \quad (12)$$

Here, P_T is the total power demand for the starting moment of the charge station, and f_k is the usage frequency index of the vehicles. In this study, P_T was considered constant. For the f_k value, half of the vehicles labeled as prosumer and consumer are set as 0.95 and the other half is set as 1.05. The flow diagram of the low-power application carried out in this study is given in Figure 9.

The designed charging station was tested using 12V-5ah 4 batteries, representing 2 manufacturer and 2 consumer labelled vehicles. The low power designed charging station model with common DC busbar is given in Figure 10.

Before the experimental study, the current load curve obtained by scaling the 24 hours of real data at a ratio of 1:16 was integrated into the software as array. The study was carried out for total of 90 minutes, considering the capacity of the batteries. The peak time period was determined as 1900-3100 seconds considering the load curve. The same scenario was repeated for the case where all vehicle batteries were charged with the nominal charging power and the power changes were compared. The current change obtained as a result of the controlled experimental study is given in Figure 11 (a).

The %SOC changes obtained as a result of the controlled operation are given in Figure 11 (b). Accordingly, during the peak time interval, 2 vehicles labeled as prosumers with fully charged batteries provided energy to 2 vehicles labeled as consumers at 60% and 65% respectively.

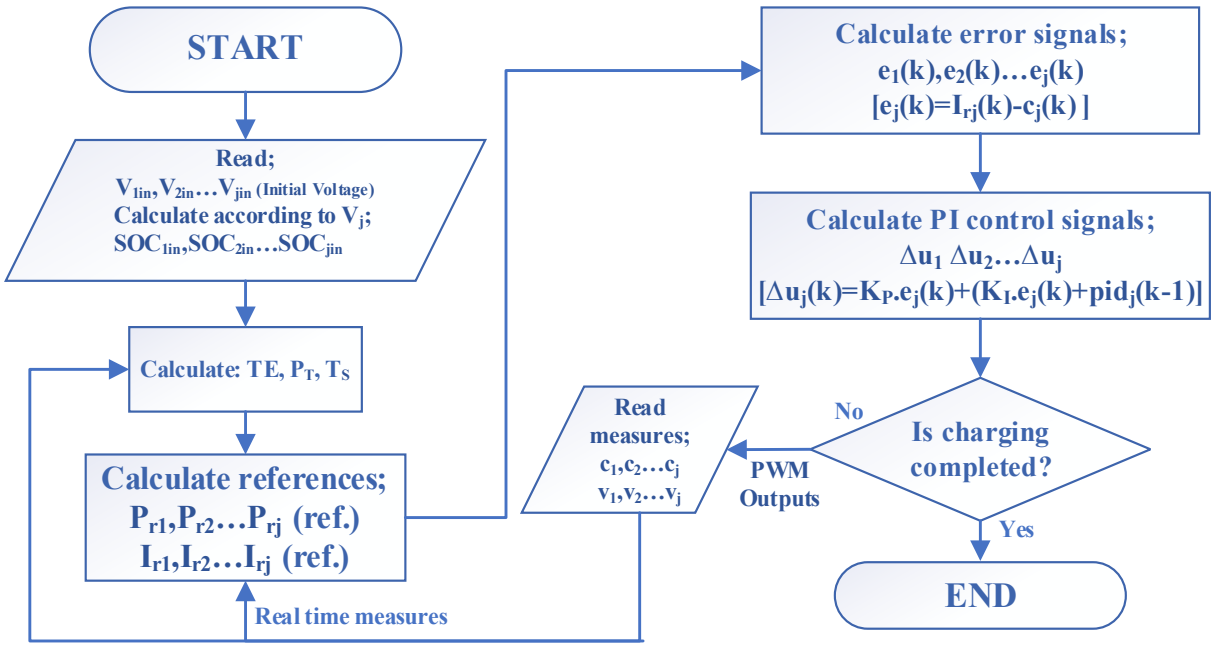

Figure 9. Power flow control flowchart

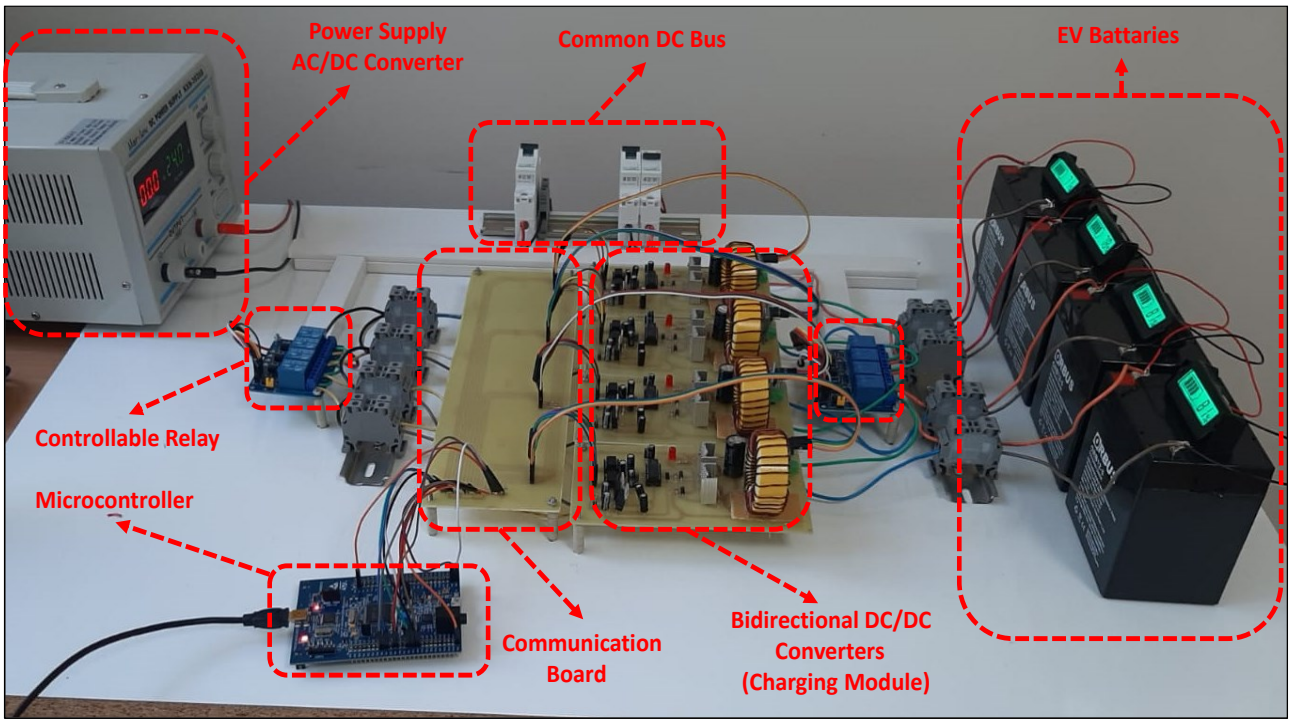

Figure 10. Prototype DC charging station

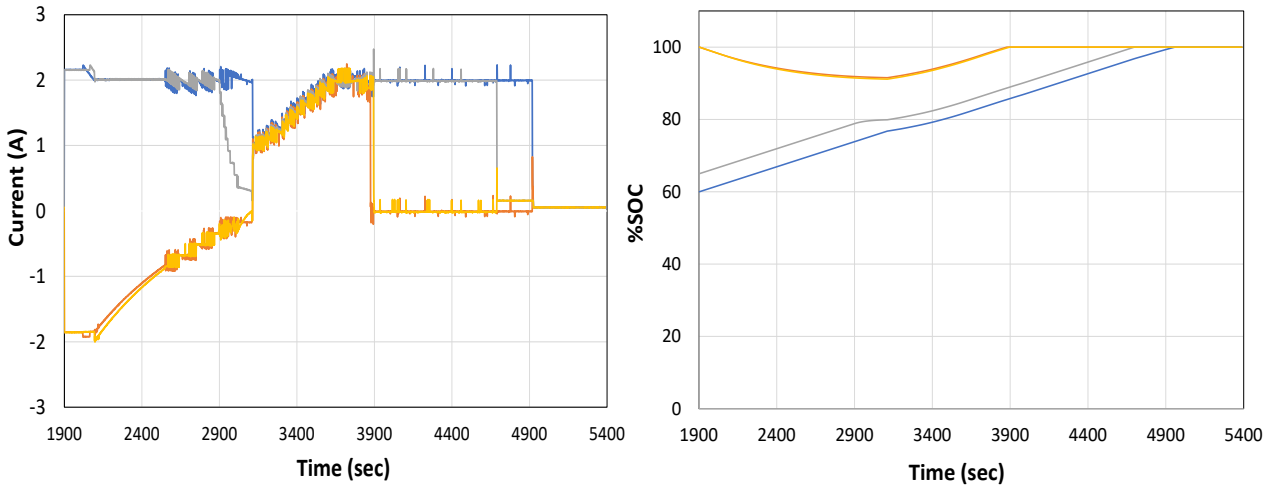

(a) (b)

Figure 11. (a) Current variations (b) %SOC changes

The most critical issue here is that the instantaneous production amount does not exceed the consumption amount at any time. This was checked while generating the references. In this way, the DC bus voltage remained constant at 24 volts throughout the run and operational stability was ensured.

Controlled and uncontrolled power variations, standard deviation and mean are given in Figure 12 (a). Figure 12 (b) shows the amount of energy shifted graphically. Accordingly, approximately 8.75 Wh energy was shifted to the off-peak time interval. Figure 12 (c) shows the load graph of the EVs on the grid within the peak hour interval in case of uncontrolled charging. Figure 12 (d) shows the Z-score frequency changes.

When the graphs are analyzed, it is understood that the power fluctuation increases even more in the case of uncontrolled charging. In addition, the standard deviation in the current load curve has also been reduced. When Figure 12 (b) and Figure 12 (c) are examined, it is understood that 54.16% of the EVs load in the peak hour range is shifted to the off-peak interval with the V2V topology.

When the graphs are analyzed, it is possible to flow energy between vehicles with the DC bus charging station infrastructure. This will enable the development of algorithms that will contribute to voltage and frequency stability on the main grid.

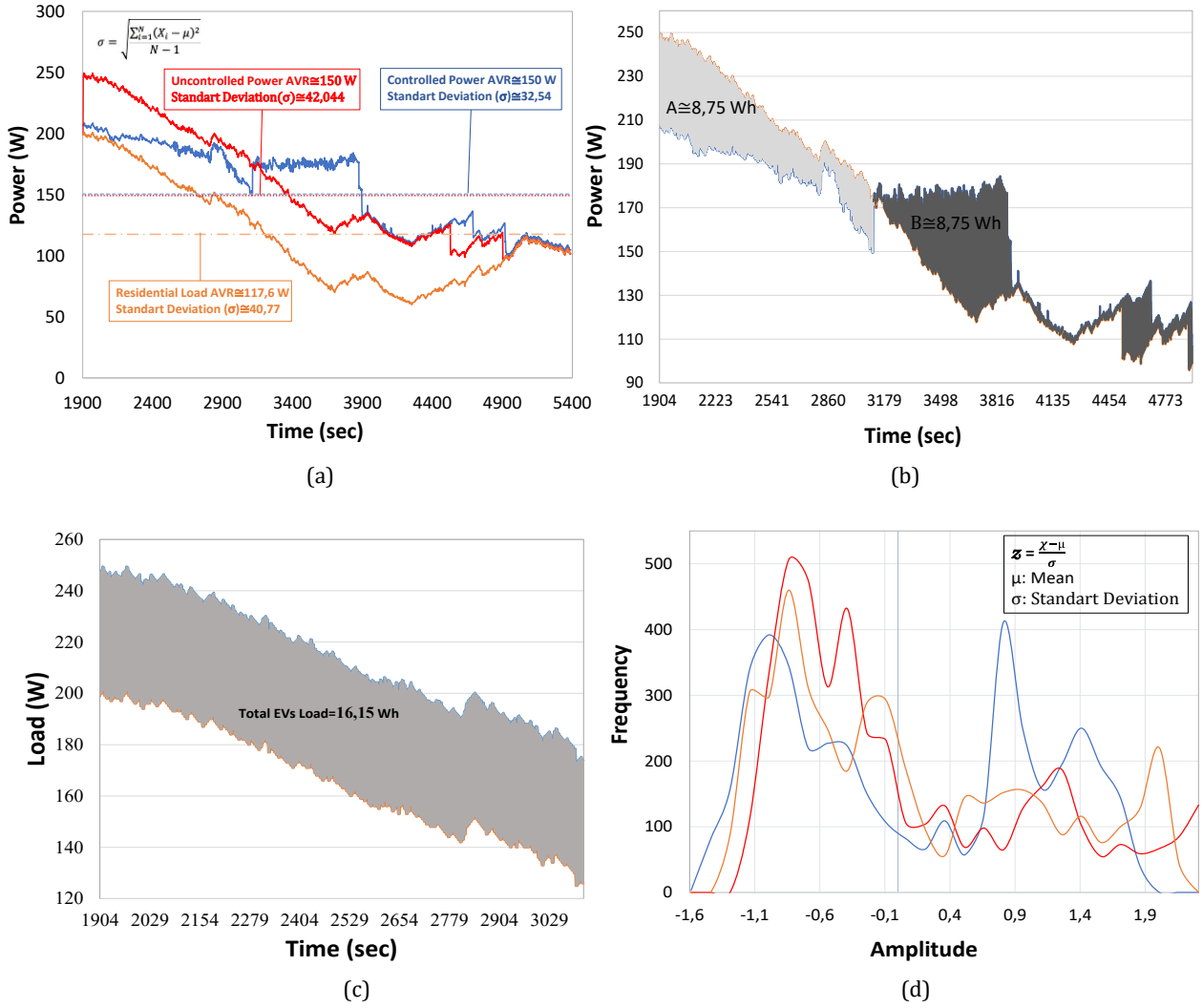

Figure 12. (a) Instantaneous power changes (b) Variation of the shifted load (c) EVs load during peak hours in uncontrolled operation (d) Z-Score frequency

5. Conclusions

In this paper, a low cost and high efficiency non-isolated bidirectional 120W DC-DC converter is designed and experimental results are presented. In addition, a low power real charging station architecture for V2V topology is presented for the first time in this work. In addition, it is proved for the first time in this study that the energy flow between vehicles can be provided in a stable manner using V2V topology. Thus, the real-world applicability of these topologies is presented for the first time.

As a result of simulation and experimental analysis of the designed DC-DC converter, it was revealed that it operates with 95% efficiency. Thus, it has been demonstrated that it is possible to produce technically feasible and highly efficient charging units for DC charging stations. However, the converter design presented in this paper is low power and fluctuations in output current variations are observed. For this reason, isolated and high-power versions of the designed converter can be used industrially.

In this sense, the high-efficiency bidirectional DC-DC converter design presented in this study will be a source of inspiration for future work.

With the low power application, it is understood that the V2V topology can be implemented stably. In this application, it is shown that 54.16% of the load of the EVs in the peak time interval is shifted to the off-peak interval by using the charge coordination strategy based on the balancing principle. Considering that the number of prosumer-consumer vehicles is equal in this application, it is understood that this ratio will be higher in case studies where the number of prosumers is higher.

As a result, not only a highly efficient bidirectional converter has been designed but also a real implementation of the V2V topology has been realised in a stable manner for the first time.

In future studies, new charge control algorithms can be developed on different cases inspired by this study.

However, the developed algorithms can be tested in industrial areas.

Acknowledgements

Funding: This study (BAP Project Number: FDK-2021-7261) was supported by Gazi University Scientific Research Projects Unit.

References

[1] Üstünsoy, F., Sayan, H.H. 2021. Real-time realization of network integration of electric vehicles with a unique balancing strategy. Electrical Engineering, 103, 2647–2660.

[2] Yildiz, S., Sayan, H.H. 2024. LCL Filter Design and Simulation for Vehicle-To-Grid (V2G) Applications. In: IMSS 2023.

[3] Mumtaz, F., Yahaya, N. Z., Meraj, S. T., Singh, B., Kannan, R., Ibrahim, O. 2021. Review on non-isolated DC-DC converters and their control techniques for renewable energy applications. Ain Shams Engineering Journal, 12(4), 3747-3763.

[4] Sahbani, A., Cherif, K., Saad, K. B. 2020. Multiphase Interleaved Bidirectional DC-DC Converter for Electric Vehicles and Smart Grid Applications. International Journal of Smart Grid-ijSmartGrid, 4(2), 80-87.

[5] Rezaii, R., Nilian, M., Safayatullah, M., Ghosh, S., & Batarseh, I. 2021. A Bidirectional DC-DC Converter with High Conversion Ratios for the Electrical Vehicle Application. In IECON 2021–47th Annual Conference of the IEEE Industrial Electronics Society, 1-6.

[6] Elserougi, A., Abdelsalam, I., Massoud, A., Ahmed, S. 2019. A bidirectional non-isolated hybrid modular DC–DC converter with zero-voltage switching. Electric Power Systems Research, 167, 277-289.

[7] Hernandez, F. D., Samanbakhsh, R., Mohammadi, P., Ibanez, F. M. 2021. A dual-input high-gain bidirectional DC/DC converter for hybrid energy storage systems in DC grid applications. IEEE Access, 9, 164006-164016.

[8] Suresh, K., Bharatiraja, C., Chellammal, N., Tariq, M., Chakrabortty, R. K., Ryan, M. J., Alamri, B. 2021. A multifunctional non-isolated dual input-dual output converter for electric vehicle applications. IEEE Access, 9, 64445-64460.

[9] Al-Obaidi, N. A., Abbas, R. A., & Khazaal, H. F. 2022. A review of non-isolated bidirectional DC-DC converters for hybrid energy storage system. In 2022 5th International Conference on Engineering Technology and its Applications (IICETA), 248-253.

[10] Pramanik, R., Pati, B. B. 2023. Modelling and control of a non-isolated half-bridge bidirectional DC-DC converter with an energy management topology applicable with EV/HEV. Journal of King Saud University-Engineering Sciences, 35(2), 116-122.

[11] Varesi, K., Hosseini, S. H., Sabahi, M., Babaei, E., Vosoughi, N. 2017. Performance and design analysis of an improved non-isolated multiple input buck DC–DC converter. IET Power Electronics, 10(9), 1034-1045.

[12] Shayeghi, H., Pourjafar, S., Hashemzadeh, S. M. 2021. A switching capacitor based multi-port bidirectional DC–DC converter. IET Power Electronics, 14(9), 1622-1636.

[13] Punna, S., Manthati, U. B., Chirayarukil Raveendran, A. 2021. Modeling, analysis, and design of novel control scheme for two-input bidirectional DC-DC converter for HESS in DC microgrid applications. International Transactions on Electrical Energy Systems, 31(10), e12774.

[14] Saadatizadeh, Z., Chavoshipour Heris, P., Sabahi, M., Tarafdar Hagh, M., Maalandish, M. 2018. A new non-isolated free ripple input current bidirectional DC-DC converter with capability of zero voltage switching. International Journal of Circuit Theory and Applications, 46(3), 519-542.

[15] Qi, X., Wang, Y., Wang, Y., Chen, Z. 2021. Optimization of centralized equalization systems based on an integrated cascade bidirectional DC–DC converter. IEEE Transactions on Industrial Electronics, 69(1), 249-259.

[16] Khan, M. A., Ahmed, A., Husain, I., Sozer, Y., Badawy, M. 2015. Performance analysis of bidirectional DC–DC converters for electric vehicles. IEEE transactions on industry applications, 51(4), 3442-3452.

[17] De Melo, R. R., Tofoli, F. L., Daher, S., Antunes, F. L. M. 2020. Interleaved bidirectional DC–DC converter for electric vehicle applications based on multiple energy storage devices. Electrical Engineering, 102, 2011-2023.

[18] Bahravar, S., Abbaszadeh, K., Olamaei, J. 2021. High step-up non-isolated DC–DC converter using diode–capacitor cells. Iranian Journal of Science and Technology, Transactions of Electrical Engineering, 45, 81-96.

[19] Cheng, X. F., Liu, C., Wang, D., Zhang, Y. 2021. State-of-the-art review on soft-switching technologies for non-isolated DC-DC converters. IEEE Access, 9, 119235-119249.

[20] Dutta, S., Rathore, A., Khadkikar, K. V., Zeineldin, H. 2021. Single-Phase Bridgeless Cuk-Derived DC-DC Converter for Vehicle-to-Vehicle Charge Transfer. *IEEE Transportation Electrification Conference (ITEC-India)*, New Delhi, India, 1-6.

[21] Artal-Sevil, J. S., Ballestín-Bernad, V., Anzola, J., Domínguez-Navarro, J. A. 2021. High-Gain Non-isolated DC-DC Partial-Power Converter for Automotive Applications. *IEEE Vehicle Power and Propulsion Conference (VPPC)*, Gijon, Spain, 1-6.

[22] Halder, T. 2023. Modelling and Simulation of a Bi-Directional DC to DC Converter System. *2nd Edition of IEEE Delhi Section Flagship Conference (DELCON)*, Rajpura, India, 1-6.

[23] Camara, M.B., Gualous, H., Gustin, F. 2010. DC/DC converter design for supercapacitor and battery power management in hybrid vehicle applicationspolynomial control strategy. IEEE Trans. Ind. Elect. 57 (2), 587–597.